

Superconductivity of Au-Ge-Yb Approximants with Tsai-type Clusters

Kazuhiko Deguchi^{1*}, Mika Nakayama¹, Shuya Matsukawa¹, Keiichiro Imura¹,
Katsumasa Tanaka², Tsutomu Ishimasa², and Noriaki K. Sato¹

¹*Department of Physics, Graduate School of Science, Nagoya University, Nagoya 464-8602, Japan*

²*Division of Applied Physics, Graduate School of Engineering, Hokkaido University, Sapporo 060-8628, Japan*

We report the emergence of bulk superconductivity in $\text{Au}_{64.0}\text{Ge}_{22.0}\text{Yb}_{14.0}$ and $\text{Au}_{63.5}\text{Ge}_{20.5}\text{Yb}_{16.0}$ below 0.68 and 0.36 K, respectively. This is the first observation of superconductivity in Tsai-type crystalline approximants of quasicrystals. The Tsai-type cluster center is occupied by Au and Ge ions in the former approximant, and by an Yb ion in the latter. For magnetism, the latter system shows a larger magnetization than the former. To explain this observation, we propose a model that the cluster-center Yb ion is magnetic. The relationship between the magnetism and the superconductivity is also discussed.

Quasicrystals (QCs) have been classified as the third solid because they possess long-range, quasi-periodic structures with diffraction symmetries forbidden for crystals. Owing to the considerable progress since the discovery of QCs in resolving their geometric structure,^{1–3} QCs are nowadays considered as a type of crystal. For their electronic structure, on the other hand, no long-range magnetic ordering has been observed although there are a few reports on superconductivity.^{4,5} For a periodic approximant crystal (AC), a phase whose composition is close to that of the QC and whose unit cell has atomic decorations similar to those of the QC, there are some reports on ferromagnetic or antiferromagnetic orderings. However, superconductivity has not been discovered thus far to the best of our knowledge.

Recently, new types of magnetic QC and AC has been discovered: the Au-Al-Yb (AAY) QC exhibits novel quantum critical behavior as observed in Yb-based heavy-fermion materials with intermediate Yb valence,⁶ while the AAY AC shows heavy-Fermi-liquid behavior. Since the diverging behavior of magnetic susceptibility as $T \rightarrow 0$ was only observed in the QC, the quantum critical state may correspond to an electronic state unique to the QCs, i.e., a critical state that is neither extended nor localized.

In the course of our research on the above novel phenomena, we learned from our review of the literature that the Au-Ge-Yb (AGY) system belongs to the 1/1 AC of a Tsai-type icosahedral QC. According to Lin and Corbett,⁷ the AGY system has two types of crystal structure: one contains 14 at% Yb and the other 16 at% Yb atoms. Almost four non-Yb (i.e., Au and Ge) atoms occupy the center of the Tsai-type cluster in the former compound as in the case of AAY,⁸ while, in the latter one, there is only a “rattling” Yb atom at the center of the cluster.⁹

Hereafter, the former and latter ACs are referred to as AGY(I) and AGY(II), respectively.

In this Letter, we report on our low-temperature experiments on the electrical resistivity, magnetization, ac magnetic susceptibility, and specific heat of the AGY(I) and AGY(II) ACs. We observe that both of the ACs show superconductivity with transition temperatures T_c of 0.68 K for AGY(I) and 0.36 K for AGY(II). We further observe that the magnetization is much larger in the AGY(II) AC than in the AGY(I) AC. To explain this observation, we propose a model in which the cluster-center Yb ion in AGY(II) is magnetic. We also discuss the relationship between magnetism and superconductivity in these new systems.

Two types of polycrystalline sample, $\text{Au}_{86-x}\text{Ge}_x\text{Yb}_{14}$ ($20 \leq x \leq 24$) and $\text{Au}_{84-y}\text{Ge}_y\text{Yb}_{16}$ ($18 \leq y \leq 22$), were synthesized with the starting materials 4N (99.99% pure)-Au, 5N-Ge, and 3N-Yb. (Note that the composition is nominal throughout the paper.) For both alloys, the starting materials were put in an alumina crucible, sealed in an evacuated quartz tube, and heated to 1000 °C. Then, the crucible was cooled to 800 °C. After it was subsequently cooled slowly to 450 °C, the crucible was rapidly quenched in water for the synthesis of AGY(I), while it was slowly cooled in the furnace for the synthesis of AGY(II).

Structure analysis was carried out by a powder X-ray diffraction technique using Cu $K\alpha$ -radiation; details of the experiments are described elsewhere.⁸ The dc magnetization was measured using a commercial SQUID magnetometer in the temperature range between 1.8 and 300 K, and at magnetic fields of up to 70 kOe. Four-terminal resistivity measurements were performed using ac methods. Ac magnetic susceptibility was measured using a driving ac magnetic field of 0.1 Oe at a frequency of 100.3 Hz. The specific heat measurement was performed by

*E-mail: deguchi@edu3.phys.nagoya-u.ac.jp

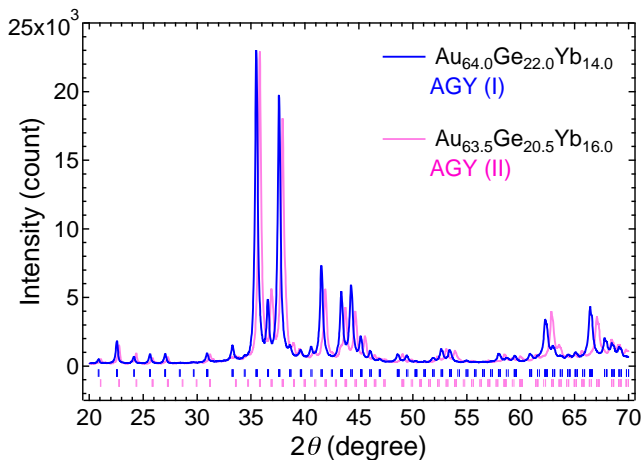


Fig. 1. (Color online) Powder X-ray diffraction patterns of $\text{Au}_{64.0}\text{Ge}_{22.0}\text{Yb}_{14.0}$ [AGY(I)] and $\text{Au}_{63.5}\text{Ge}_{20.5}\text{Yb}_{16.0}$ [AGY(II)]. Note that the spectrum slightly shifts from each other due to the difference in the lattice parameter. The peak positions of AGY(I) and AGY(II) are denoted by bars in the upper and lower regions, respectively.

a conventional quasi-adiabatic heat-pulse method. The electrical resistivity, ac magnetic susceptibility, and specific heat measurements with zero dc magnetic field were carried out in a ^3He cryostat down to 0.25 K, and the resistivity and ac magnetic susceptibility measurements at magnetic fields of up to 80 kOe were carried out in a dilution refrigerator down to 0.08 K.

Figure 1 shows the powder X-ray diffraction patterns of $\text{Au}_{64.0}\text{Ge}_{22.0}\text{Yb}_{14.0}$ and $\text{Au}_{63.5}\text{Ge}_{20.5}\text{Yb}_{16.0}$, both of which show a body-centered cubic structure with lattice parameters of 1.4724(2) and 1.4605(4) nm, respectively. Note that the alloy with a higher Yb concentration has a smaller lattice parameter, as pointed out in Ref. 7.

The Rietveld structure analysis of the former successfully converged and indicated that the sample with an optimal composition $x = 64.0$ is of single phase and its cluster-center tetrahedron is orientationally disordered.¹⁰ For the latter, on the other hand, the predominant phase has an optimal composition of $y = 63.5$ and the sample contains a small amount of an unidentified phase. The inclusion of the secondary phase prevented the complete Rietveld refinement. In the present study, we assume following Lin and Corbett that, there is a single Yb atom at the cluster center in the latter system.^{7,9} As a result, AGY(I) and AGY(II) denote $\text{Au}_{64.0}\text{Ge}_{22.0}\text{Yb}_{14.0}$ and $\text{Au}_{63.5}\text{Ge}_{20.5}\text{Yb}_{16.0}$, respectively.

Figure 2 shows two structure models, both of which are composed of the Tsai-type cluster, i.e., concentric shells of a dodecahedron, an icosahedron, and an icosidodecahedron. Note that the “Yb1” site at the vertex of the icosahedron is exclusively occupied by the Yb atom. The structure model of the AGY(I) AC is similar to that of

the AAY AC; the cluster center is occupied by Au atoms with a probability of approximately 0.27 (Ref. 10), which is close to 1/3 in the case of a randomly oriented tetrahedron. In contrast, in the structure model of the AGY(II) AC, the cluster center is occupied by a single Yb atom (“Yb2” site).

Figure 3(a) shows the temperature dependences of the magnetic susceptibilities of the AGY(I) and AGY(II) ACs. For comparison, we also plot the susceptibility data of the AAY AC.⁶ For the analysis described below, the magnetic susceptibilities of AGY(I) and AGY(II) ACs are plotted in unit per cluster (see the left vertical axis), including 12 and 13 Yb atoms, respectively, while that of the AAY AC is given in unit per Yb ion (the right vertical axis). The AGY(I) AC shows an almost T -independent diamagnetic susceptibility $\chi = -1.6 \times 10^{-4}$ emu/mol-cluster at high temperatures, and shows a Curie-like rise in $\chi(T)$ in the lowest-temperature region measured. The latter rise seems extrinsic because the low-temperature magnetization $M(H)$ saturates at a low magnetic field; as shown in Fig. 3(b), $M(H)$ is only $9.6 \times 10^{-3} \mu_B/\text{cluster}$ at $H = 50$ kOe. It is reasonable to assume that the T -constant diamagnetism arises as a result of the cancellation between the paramagnetic contribution of conduction electrons and the diamagnetic contribution of ion cores. Since the latter susceptibility is estimated to be $\sim -1.8 \times 10^{-3}$ emu/mol-cluster from the ion core susceptibility given in the literature,¹¹ the Pauli susceptibility is evaluated as $\sim 1.6 \times 10^{-3}$ emu/mol-cluster. Using a measured electronic-specific-heat coefficient $\gamma = 109$ mJ/K²mol-cluster, we obtain a Wilson ratio $R_W = \pi^2 k_B^2 \chi / 3 \mu_B^2 \gamma \sim 1$, which is expected for a noncorrelated electron system. As a result, the observed magnetism of the AGY(I) AC can be understood by assuming that all the Yb ions (i.e., the Yb1-site ions at the vertex of the icosahedron) are in the nonmagnetic Yb^{2+} state.¹²

In contrast, the magnetic susceptibility of the AGY(II) AC (containing both the Yb1- and Yb2-site ions) behaves like that of the AAY AC. Assuming that $\chi(T) = \chi_0 + \chi_{4f}(T)$ [χ_0 and $\chi_{4f}(T)$ are T -independent and T -dependent contributions to the susceptibility, respectively], we find that, for $T > 80$ K, $\chi_{4f}(T)$ follows the Curie-Weiss law with an effective Bohr magneton $\mu_{\text{eff}} = 3.5 \mu_B/\text{cluster}$ and a Weiss temperature $T_\theta = 104$ K. Note that this effective magnetic moment per cluster is close to $3.8 \mu_B/\text{Yb}$ of the AAY AC. Since the constant term $\chi_0 = 4.8 \times 10^{-3}$ emu/mol-cluster is also considered as additive contributions of conduction electrons and ion cores, the Pauli paramagnetism of the AGY(II) AC is estimated to be $\sim 6.8 \times 10^{-3}$ emu/mol-cluster from the ion core diamagnetism of $\sim -2.0 \times 10^{-3}$ emu/mol-cluster. Assuming $\gamma \sim 251$ mJ/K²mol-cluster at high temperatures, we obtain a Wilson ratio $R_W \sim 2$, which suggests the possibility that the $4f$ electrons would contribute to the itinerant electron magnetism.

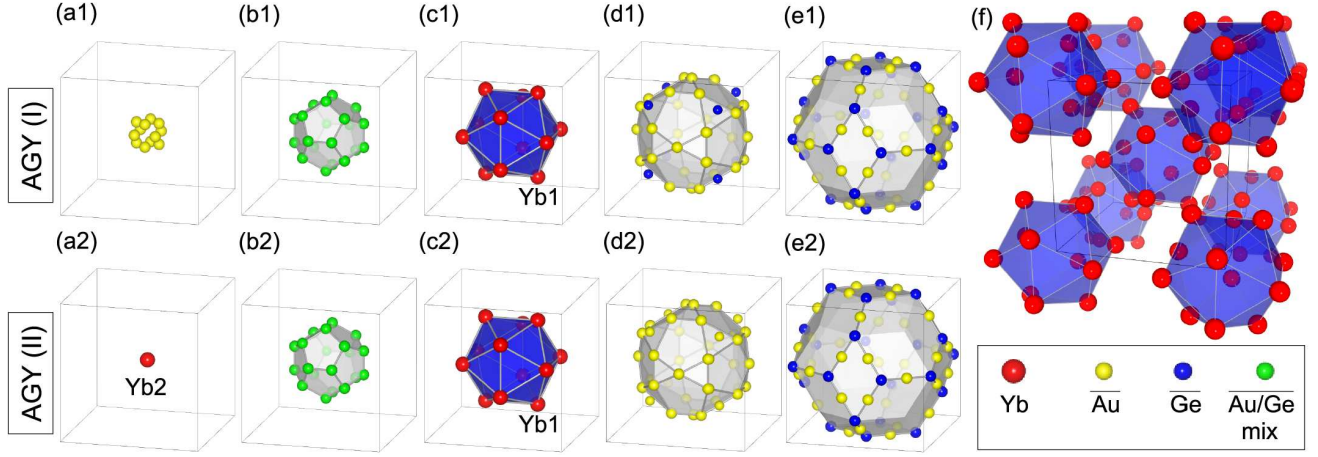


Fig. 2. (Color online) Concentric shell structure of Tsai-type cluster. (a1)-(e1) are for AGY(I), and (a2)-(e2) are for AGY(II). The square frame is a unit cell. The sites including Au and Ge are classified into three groups: $\overline{\text{Au}}$ (more than 90% Au), $\overline{\text{Ge}}$ (more than 90% Ge), and mixed Au/Ge (other). (a1) Orientationally disordered tetrahedron with $\overline{\text{Au}}$ atoms. (a2) Single Yb ion at the center of the cluster (Yb2 site). (b1),(b2) Second shell of dodecahedron composed of mixed Au/Ge atoms. (c1),(c2) Third shell of icosahedron with Yb ions on the vertex (Yb1 sites). (d1),(d2) Fourth shell of icosidodecahedron with $\overline{\text{Au}}$ atoms. The atom centered at $[1/4\ 1/4\ 1/4]$ is Ge or Au. (e1),(e2) Fifth shell of triacontahedron with $\overline{\text{Au}}$ and $\overline{\text{Ge}}$ atoms. (f) Body-centered cubic arrangement of the icosahedron in the Au-Ge-Yb AC.

Let us make a comparison between the AGY(II) AC and the AAY AC. The solid line in Fig. 3(a) indicates that $\chi_{4f}(T) = a\chi_{\text{AAY}}(T)$, where a is an adjustable parameter and found to be 0.9 and $\chi_{\text{AAY}}(T)$ is a measured susceptibility (per mole of Yb ion) of the AAY AC. We find good coincidence between the solid curve and the data points, suggesting that Yb ions in the AGY(II) AC are similar in nature to those in the AAY AC.

Figure 3(b) shows the magnetization curves for the AGY(I), AGY(II), and AAY ACs. We ascribe the small magnetization of the AGY(I) AC to a paramagnetic impurity effect. The solid line indicates that $M(H) = \chi_0 H + M_{4f}(H)$, where $M_{4f}(H) = aM_{\text{AAY}}(H)$ [$a = 0.9$ and $M_{\text{AAY}}(H)$ is a measured magnetization of the AAY AC per Yb ion]. Again, we find good agreement between the solid curve and the data points. Taking account of the results (i) that the magnetization per cluster (containing 12 Yb1-site ions and 1 Yb2-site ion) in the AGY(II) AC is similar in magnitude to that per Yb ion in the AAY AC and (ii) that 12 Yb1-site ions are all nonmagnetic in the AGY(I) AC, we propose a model showing that, in the AGY(II) AC, the Yb1-site Yb ions are all nonmagnetic and the Yb2-site Yb ion behaves like the Yb ions in the AAY AC. This implies that the AGY(II) AC has a heterogeneous Yb valence.

Figure 4(a) shows the temperature dependences of the electrical resistivities $\rho(T)$ of the AGY(I) and AGY(II) ACs. The T -independent feature with a large residual resistivity [see inset of Fig. 4(a)] is characteristic of ACs as well as QCs with Tsai-type clusters. The electrical resistivities of both materials sharply drop to zero, indicating the emergence of superconductivity. By defining

the transition temperature T_c as the midpoint of the resistivity drop, we obtain $T_c = 0.68$ and 0.36 K for the AGY(I) and AGY(II) ACs, respectively.

Figure 4(b) shows the temperature dependences of the real parts of the ac magnetic susceptibilities $\chi'(T)$ of the AGY(I) and AGY(II) ACs with zero external dc magnetic field. Below T_c , there emerges a clear diamagnetic signal due to the superconducting shielding effect. When defining T_c as the onset of diamagnetism, we find that the T_c values deduced from the susceptibility and resistivity coincide with each other.

Detailed studies of the field-dependent resistivity and ac susceptibility allow us to determine the upper critical field $H_{c2}(T)$; see the inset of Fig. 4(b). Just below T_c , we observe a linear T dependence with gradients of $dH_{c2}/dT = 5.84$ and 6.75 kOe/K for the AGY(I) and AGY(II) ACs, respectively. The orbital critical field at zero temperature is estimated using this slope via the Werthamer-Helfand-Hohenberg formula $H_{c2}^{\text{orb}}(0) = -0.693T_c dH_{c2}/dT$, and the results are summarized in Table I, together with the $H_{c2}(0)$ values obtained by extrapolating the data to zero temperature. We find that $H_{c2}^{\text{orb}}(0)$ is close to $H_{c2}(0)$ for both materials, suggesting that the orbital depairing mechanism dominantly contributes to the H_{c2} of these ACs.

To check if the superconductivity is of bulk origin, we measured the specific heat $C(T)$. In the normal state, $C(T)$ can be well fitted using the conventional formula $C(T) = \gamma T + \beta T^3$ ($2 < T < 5$ K) with $\gamma = 109$ and 251 mJ/K²mol-cluster, and $\beta = 40.8$ and 41.1 mJ/K⁴mol-cluster for the AGY(I) and AGY(II) ACs, respectively. Using $\beta = 12\pi^4 NR/5\Theta_D^3$ (R is the gas constant and N

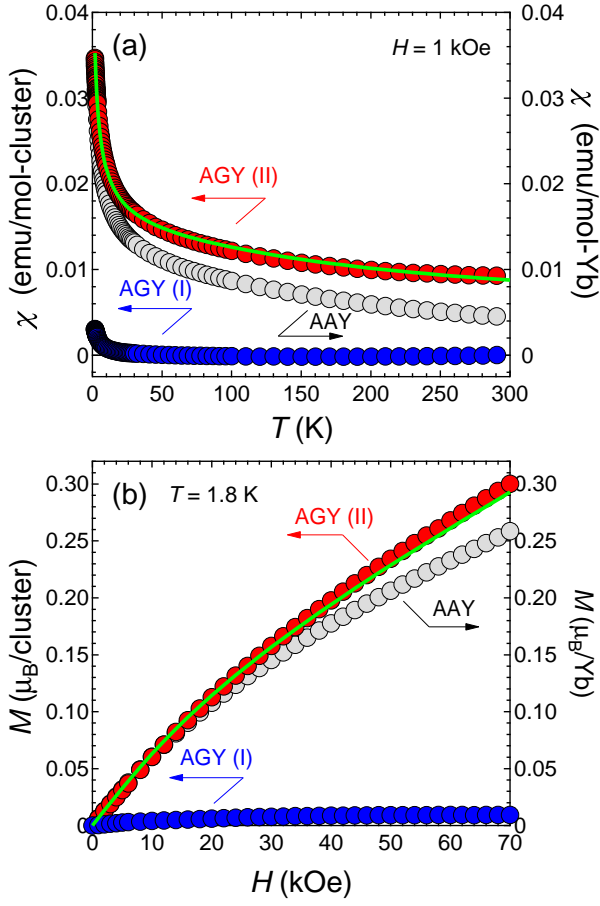


Fig. 3. (Color online) (a) Dc magnetic susceptibilities $\chi(T)$ of the AGY(I), AGY(II), and AAY ACs measured at $H = 1$ kOe. (b) Magnetization curves $M(H)$ for the AGY(I), AGY(II), and AAY ACs at $T = 1.8$ K. Solid lines in (a) and (b) indicate calculated results; see text for details.

is the number of atoms), we estimate the Debye temperature to be $\Theta_D = 160$ and 157 K for the AGY(I) and AGY(II) ACs, respectively. Then, by subtracting the phonon contribution of $C(T)$, we evaluate the electronic specific heat $C_e(T)$. In Fig. 4(c), we plot C_e/T as a function of temperature. A clear jump is observed at T_c : the thin solid line indicates the T dependence calculated using entropy balance. The jump height is $\Delta C_e/T_c = 138$ and 218 mJ/K²mol-cluster and therefore $\Delta C_e/C_e(T_c)$ is 1.26 and 0.54 for the AGY(I) and AGY(II) ACs, respectively. These values indicate the bulk superconductivity and suggest that, if the $4f$ electrons would be itinerant, then they are involved in Cooper pair formation.

In the normal state, the AGY(II) AC shows a logarithmic increase in C_e/T at low temperatures in contrast to the AGY(I) AC: the solid line in Fig. 4(c) indicates a fitted result using the expression $C_e/T \sim -(S^*/T^*) \ln(T/T^*)$ with $T^* = 33$ K and $S^* = 2860 = 0.5R \ln 2$ mJ/Kmol-cluster. Such a logarithmic T depen-

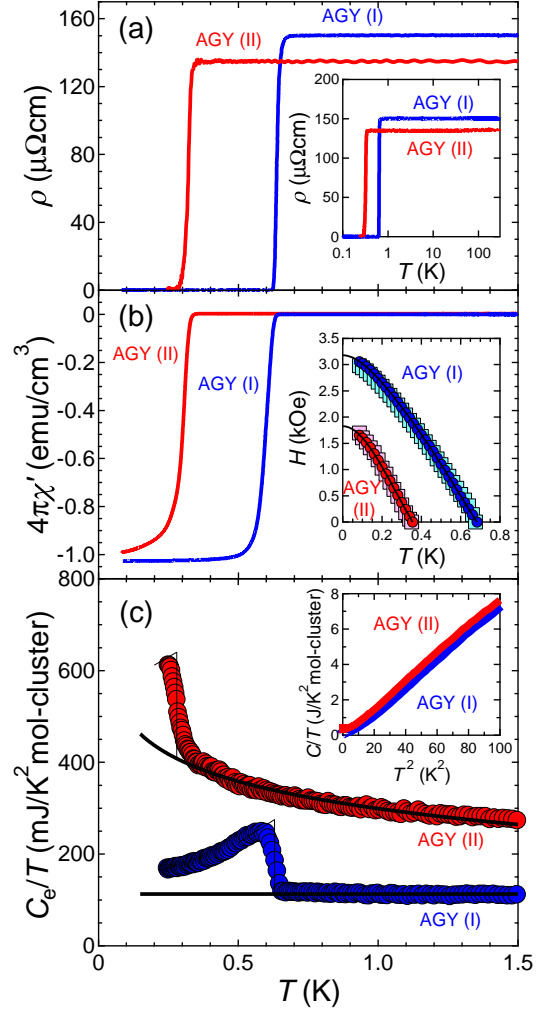


Fig. 4. (Color online) (a) Electrical resistivities $\rho(T)$ of the AGY(I) and AGY(II) ACs. The inset shows the electrical resistivity on a logarithmic abscissa for $0.1 < T < 300$ K. (b) Real parts of the ac magnetic susceptibilities $\chi'(T)$ of the AGY(I) and AGY(II) ACs. The absolute value was calibrated with the superconductivity of Pb ($T_c = 7.2$ K). The inset shows the upper critical field $H_{c2}(T)$ of the AGY(I) and AGY(II) ACs deduced from the ac magnetic susceptibility (open squares) and resistivity (open circles). Solid lines are a guide for the eyes. (c) Electronic specific heat divided by temperature C_e/T of the AGY(I) and AGY(II) ACs. The low- T behavior in the AGY(I) AC is likely due to the nuclear contribution. The inset shows the specific heat divided by temperature C_e/T versus T^2 for the AGY(I) and AGY(II) ACs.

dence was observed in UPt_3 ,¹³ which allows us to suggest the possibility of an unconventional pairing mechanism related to the magnetism.

The superconducting parameters of these materials are summarized in Table I. They are evaluated using the knowledge of T_c , $H_{c2}(T)$ and $\Delta C_e/T_c$ as follows: The GL parameter κ at $T = T_c$ is deduced from the relation $4\pi \times 1.16 \times (2\kappa^2 - 1) \Delta C_e/T_c = (dH_{c2}/dT)^2$, and we assume that $\kappa(0) \simeq \kappa$ from $H_{c2}(0) \simeq H_{c2}^{\text{orb}}(0)$. Note that

Table I. Superconducting parameters of the AGY(I) and AGY(II) ACs. The underlined quantities were measured, and the others were calculated using theoretical relations described in the text.

Parameter	AGY(I)	AGY(II)
T_c (K)	<u>0.68</u>	<u>0.36</u>
$H_{c2}(0)$ (kOe)	<u>3.18</u>	<u>1.83</u>
$H_{c2}^{\text{orb}}(0)$ (kOe)	2.76	1.65
$H_c(0)$ (Oe)	78.7	50.0
$H_{c1}(0)$ (Oe)	6.7	4.5
$\xi(0)$ (nm)	32.2	42.4
$\lambda(0)$ (nm)	9.2×10^2	11.0×10^2
$\kappa(0)$	28.6	25.9

the large κ values exceeding 20 indicate that both materials are type II superconductors. The coherence length $\xi(0)$ is estimated from $H_{c2}(0) = \Phi_0/2\pi\xi(0)^2$, where Φ_0 is a flux quantum. The penetration depth is estimated from the relation $\lambda(0) = \kappa(0)\xi(0)$. The thermodynamic critical field is evaluated from $H_c(0) = H_{c2}(0)/\sqrt{2}\kappa(0)$. Finally, the lower critical field is estimated using the formula $H_{c1}(0)H_{c2}(0) = H_c(0)^2(\ln\kappa(0) + 0.08)$. As seen in Table I, we find no clear difference in the superconducting parameter, $\xi(0)$, $\lambda(0)$, or $\kappa(0)$ for the AGY(I) or AGY(II) AC.

We consider two possibilities for the relationship between magnetism and superconductivity: (i) The superconductivity mechanisms are different between AGY(I) and AGY(II), and the magnetism stabilizes the superconductivity for the latter. (ii) The superconductivity mechanism is common between them and the magnetism destabilizes the superconductivity for the latter. At the present stage, it is unclear which of those possibilities is probable: we need further investigations.

In summary, we synthesized two Tsai-type 1/1 ACs with a nominal composition, $\text{Au}_{64.0}\text{Ge}_{22.0}\text{Yb}_{14.0}$ [AGY(I)] and $\text{Au}_{63.5}\text{Ge}_{20.5}\text{Yb}_{16.0}$ [AGY(II)]. By low-temperature experiments on their electrical resistivity, magnetization, ac magnetic susceptibility, and specific heat, we showed that they are the first superconductors among Tsai-type QCs and ACs. To account for the different magnetic properties of AGY(I) and AGY(II) ACs,

we proposed a model in which Yb ion located at the Tsai-type cluster center, which exists only in the AGY(II) AC, is magnetic while the other Yb ions located at the vertex of the icosahedron are nonmagnetic. We further discussed the possible effect of the cluster-center magnetic Yb ion on superconductivity. We hope that the present study stimulates further search for superconducting QC and AC, and research on the relationship between magnetism and superconductivity as well.

Acknowledgments

The authors thank S. Watanabe and K. Miyake for valuable discussions. This work was partially supported by Grants-in-Aid for Scientific Research from JSPS, KAKENHI (Nos. 24654102, 25610094, and 26610100). K.D. also thanks the Yamada Science Foundation for financial support.

- 1) D. Shechtman, I. Blech, D. Gratias, and J. W. Cahn: Phys. Rev. Lett. **53** (1984) 1951.
- 2) A. P. Tsai, J. Q. Guo, E. Abe, H. Takakura, and T. J. Sato: Nature **408** (2000) 537.
- 3) H. Takakura, C. P. Gomez, A. Yamamoto, M. de Boissieu, and A. P. Tsai: Nat. Mater. **6** (2007) 58.
- 4) K. M. Wong, E. Lopdrup, J. L. Wagner, Y. Shen, and S. J. Poon: Phys. Rev. B **35** (1987) 2494.
- 5) J. L. Wagner, B. D. Biggs, K. M. Wong, and S. J. Poon: Phys. Rev. B **38** (1988) 7436.
- 6) K. Deguchi, S. Matsukawa, N. K. Sato, T. Hattori, K. Ishida, H. Takakura, and T. Ishimasa: Nat. Mater. **11** (2012) 1013.
- 7) Q. Lin and J. D. Corbett: Inorg. Chem. **49** (2010) 4570.
- 8) T. Ishimasa, Y. Tanaka, and S. Kashimoto: Philos. Mag. **91** (2011) 4218.
- 9) G. H. Gebresenbut, R. Tamura, D. Eklöf, and C. P. Gómez: J. Phys.: Condens. Matter **25** (2013) 135402.
- 10) K. Deguchi, M. Nakayama, S. Matsukawa, K. Imura, K. Tanaka, T. Ishimasa, and N. K. Sato: J. Phys. Soc. Jpn. **84** (2015) 015002.
- 11) P. W. Selwood: *Magnetochemistry* (Interscience Publishers, Inc., New York, 1956).
- 12) S. Matsukawa, K. Tanaka, M. Nakayama, K. Deguchi, K. Imura, H. Takakura, S. Kashimoto, T. Ishimasa, and N. K. Sato: J. Phys. Soc. Jpn. **83** (2014) 034705.
- 13) G. R. Stewart: Rev. Mod. Phys. **56** (1984) 755.